

# GALERKIN RESIDUALS FOR ADAPTIVE SYMMETRIC-GALERKIN BOUNDARY ELEMENT METHODS

By Glaucio H. Paulino,<sup>1</sup> Associate Member, ASCE, and L. J. Gray<sup>2</sup>

**ABSTRACT:** This paper presents a simple a posteriori error estimator and an effective adaptive mesh refinement procedure for the symmetric Galerkin boundary element method. The “hypersingular residuals,” developed for error estimation in a standard collocation BEM, are extended to the symmetric Galerkin setting. This leads to the formulation of “Galerkin residuals,” which are intrinsic to the symmetric Galerkin boundary integral approach and form the basis of the present error estimation scheme. Several computational experiments are conducted to test both the accuracy and the reliability of the proposed technique. These experiments involve potential theory and various problem configurations including mixed boundary conditions, corners, and nonconvex domains. The numerical results indicate that reliable solutions to practical engineering problems can be obtained with this method.

## INTRODUCTION

For nearly 30 years, the “collocation” method [e.g., Brebbia et al. (1984), Becker (1992), and Banerjee (1994)] has been the dominant numerical approach for the solution of boundary integral equations (BIEs). Compared with the finite-element method (FEM), the advantages of the boundary element method (BEM) are easy input, high accuracy of the results, and relatively simple extension to adaptivity (e.g.,  $h$ -version, which consists of adjusting the level of mesh refinement). However, it leads to fully populated, nonsymmetric matrices. Recently, the symmetric Galerkin (SG) approximation (Hartmann et al. 1985; Sirtori et al. 1992) has emerged as a highly attractive alternative. The key advantage of Galerkin formulations is the ability to work with hypersingular integral equations using standard continuous elements (e.g., linear and quadratic). Evaluation of hypersingular integrals with collocation requires either a differentiable boundary (Gray 1993; Paulino 1995) or a nonconforming (discontinuous) (Selcuk et al. 1994) interpolation. [Recently, there has been considerable discussion on smoothness requirements for density functions in the BEM. See, for example, the papers by Martin and Rizzo (1996), and Cruse and Richardson (1997).] Differentiable interpolations using, for example, Hermite (Watson 1986; Rudolphi and Muci-Küchler 1991; Tomlinson et al. 1996) or Overhauser (Hall and Hibbs 1988) elements are difficult and computationally expensive, especially in three dimensions. The nonconforming approach [e.g., Selcuk et al. (1994)] adds significantly to the number of unknowns and is therefore also quite expensive.

Compared with collocation methods, the traditional Galerkin method is very expensive, but the added symmetric aspect makes this approach computationally efficient. Although nonsymmetric Galerkin is roughly an order of magnitude slower than collocation, SG can be as fast or faster (Balakrishna et al. 1994). Thus, the advantages of Galerkin—accuracy, standard continuous interpolation, accurate corner analysis—can be obtained without paying a price in terms of efficiency.

This paper is concerned with error estimation and adaptive procedures for use with the symmetric Galerkin method. Re-

cently, Holzer (1994) has presented a  $p$ -version (which consists of increasing the degree of the approximating piecewise polynomial trial functions) of the symmetric Galerkin BEM (SG-BEM). Essentially he has extended the numerical results of Postell and Stephan (1990) to mixed boundary value problems in potential and elasticity. Holzer (1995) has also developed  $h$ -,  $p$ -, and  $hp$ -versions (the  $hp$ -version is a combination of both the  $h$ - and  $p$ -versions) of the symmetric BEM in elasticity.

There are surveys on error estimation and adaptivity in BEM; however, most of them are on collocation methods. Examples are the articles by Kita and Kamiya (1994) and Liapis (1995). Moreover, Mackerle (1993, 1994) has compiled a list of references on mesh generation, refinement, error analyses, and adaptive techniques for both BEM and FEM. In the mathematical literature, Sloan (1990, 1992) has presented an excellent treatise of the subject; Yu (1987, 1988) and Wendland and Yu (1988, 1992) have presented local error estimates based on a linear error-residual relation that is very effective in the FEM. Their initial arguments required the restrictive assumption of uniform meshes (Yu 1987, 1988; Wendland and Yu 1988) but this was relaxed later for Galerkin methods (Wendland and Yu 1992). More recently, Carstensen (1995, 1996), Carstensen and Stephan (1995), and Carstensen et al. (1995) have presented error estimates for the BEM in a manner similar to that outlined by Eriksson et al. (1995) for the FEM. Previous work on residual type error estimates in collocation BEM also include the publications by Abe (1992), Parreira and Dong (1989), Rank (1989), Sun and Zamani (1992), and Yu (1991). Recently, Paulino et al. (1997) have used nodal sensitivities (rates of change of response quantities with respect to nodal positions) as error estimates in computational mechanics. They have also reviewed the literature on error estimation, especially estimates based on nodal perturbation schemes.

An important feature of the theory of singular integral equations is that the problem for the boundary unknowns may be formulated in different ways (e.g., Banerjee 1994). The error estimation method proposed herein relies on this feature. Thus, one may formulate two distinct boundary integral equations, e.g., the singular BIE and the hypersingular BIE (HBIE), to represent the same boundary value problem. A natural measure of the error, presented by Paulino et al. (1996), rests on the use of both the BIE and the HBIE. For instance, suppose that an approximate solution, using one of the BIEs, has been obtained. Then, one expects that the residual obtained when this approximate solution is substituted in the other BIE is related to the error. Numerical experiments have suggested that this is indeed the case (Paulino 1995; Menon 1996).

In this work, the above error estimation method, developed for the collocation BEM [e.g., Paulino et al. (1996)], is ex-

<sup>1</sup>Asst. Prof., Dept. of Civ. and Envir. Engrg., Univ. of Illinois, Urbana, IL 61801.

<sup>2</sup>Sr. Res. Staff Member, Math. Sci. Sect., Comp. Sci. and Mathematics Div., Oak Ridge Natl. Lab., P.O. Box 2008, Build. 6012, TN 37831-6367.

Note. Associate Editor: Sunil Saigal. Discussion open until October 1, 1999. To extend the closing date one month, a written request must be filed with the ASCE Manager of Journals. The manuscript for this paper was submitted for review and possible publication on December 19, 1997. This paper is part of the *Journal of Engineering Mechanics*, Vol. 125, No. 5, May, 1999. ©ASCE ISSN 0733-9399/99/0005-0575-0585/\$8.00 + \$.50 per page. Paper No. 17213.

tended to the symmetric Galerkin BEM. This method is, for two basic reasons, the natural setting for this type of residual error estimates. First, SG by definition employs both equations (i.e., the BIE and the HBIE) in the problem solution, so it is natural to think of using the alternate equation to compute a residual. Second, as mentioned above, hypersingular equations are most easily dealt with by means of a Galerkin approximation, and thus both the problem solution and the residuals can be computed in the same fashion.

The remainder of this paper is organized as follows. First, the BIEs for solving potential problems are provided, and the symmetric Galerkin method is introduced. The ‘‘Galerkin residuals’’ are then defined and their use as error estimates is discussed. An adaptive mesh refinement strategy is presented, including techniques for local and global error estimation and a criterion for element refinement. Several aspects concerning the numerical implementation of these procedures are discussed, and three numerical examples are given. Finally, conclusions and directions for future research are discussed.

## BOUNDARY INTEGRAL EQUATIONS

Consider the solution of Laplace equation in a region with mixed boundary conditions, formally stated as

$$\Delta\phi = 0 \quad \text{in } \Omega \in \mathbf{R}^2; \quad \phi = g_1 \quad \text{on } \Gamma_1 \quad (1a,b)$$

$$\mathcal{F} \equiv \frac{\partial\phi}{\partial\mathbf{n}} = g_2 \quad \text{on } \Gamma_2 \quad (1c)$$

where  $\Gamma = \Gamma_1 \cup \Gamma_2$  for a well-posed problem. The solution of the boundary value problem consists of finding  $\mathcal{F}(\partial\phi/\partial\mathbf{n} = \nabla\phi \cdot \mathbf{n})$  on  $\Gamma_1$  (Dirichlet surface) and  $\phi$  on  $\Gamma_2$  (Neumann surface). The approximate solution to the problem in (1) can be obtained by reformulating the boundary value problem as a BIE that can be solved using the standard BEM, the SG-BEM, or other alternative BEM formulations [e.g., Ghosh et al. (1986) and Nagarajan et al. (1996)]. This procedure allows the solution of problems of practical importance with irregular geometries.

In this work, all the BIEs are treated using the ‘‘limit to the boundary’’ approach (Gray 1989; Gray et al. 1990; Paulino 1995), which consists of formulating the BIE through a limit from the interior representation. This representation permits writing the same BIE for points either inside the domain or on the boundary. The boundary limit approach provides a mathematically valid interpretation of both singular and hypersingular integrals and, what is more, leads to a direct evaluation algorithm, avoiding boundary deformations, e.g., exclusion zone.

## Collocation

In the BEM context, ‘‘collocating’’ means enforcing the respective BIE in a set of points on the boundary, which are element nodal points. Within the framework described above, the singular BIE can be written in the form

$$\phi(P) + \int_{\Gamma} \frac{\partial G}{\partial\mathbf{n}}(P, Q)\phi(Q) dQ = \int_{\Gamma} G(P, Q)\mathcal{F}(Q) dQ \quad (2)$$

where  $\mathbf{n} \equiv \mathbf{n}(Q)$  is the unit normal at a point  $Q$  on the domain boundary  $\Gamma$ , and  $\partial(\cdot)/\partial\mathbf{n}$  denotes the normal derivative with respect to  $Q$ . The free-space Green function or fundamental solution is taken as the point source potential

$$G(P, Q) = -\frac{1}{2\pi} \log r \quad (3)$$

where  $r = \|\mathbf{r}\| = \|Q - P\|$ . The corresponding HBIE is obtained by differentiating (2) with respect to  $P$  in the direction  $\mathbf{N} \equiv$

$\mathbf{n}(P)$ , the normal to the boundary at  $P$  (according to the limit from the interior representation). This results in

$$\frac{\partial\phi}{\partial\mathbf{N}}(P) + \int_{\Gamma} \frac{\partial^2 G}{\partial\mathbf{N}\partial\mathbf{n}}(P, Q)\phi(Q) dQ = \int_{\Gamma} \frac{\partial G}{\partial\mathbf{N}}(P, Q)\mathcal{F}(Q) dQ \quad (4)$$

where  $\partial(\cdot)/\partial\mathbf{N}$  indicates the normal derivative with respect to  $P$ . The collocation method is inherently nonsymmetric, as the computation involves an integration for every point ( $P$ ) and element ( $Q$ ) pair.

## Symmetric Galerkin

When using the Galerkin method in a BEM context, each matrix element is a two-dimensional integral on the boundary—an outer integration with respect to  $P$  and an inner integration with respect to  $Q$ . Thus, the integral equations (2) and (4) are enforced in a weighted sense in the form

$$\begin{aligned} & \int_{\gamma_P} \psi_k(P) \int_{\Gamma_1} G(P, Q)\mathcal{F}_1(Q) dQ dP \\ & - \int_{\gamma_P} \psi_k(P) \int_{\Gamma_2} \frac{\partial G}{\partial\mathbf{n}}(P, Q)\phi_2(Q) dQ dP = \int_{\gamma_P} \psi_k(P)g_1(P) dP \\ & + \int_{\gamma_P} \psi_k(P) \int_{\Gamma_1} \frac{\partial G}{\partial\mathbf{n}}(P, Q)g_1(Q) dQ dP \\ & - \int_{\gamma_P} \psi_k(P) \int_{\Gamma_2} G(P, Q)g_2(Q) dQ dP, \quad \gamma_P \in \Gamma_1 \end{aligned} \quad (5)$$

and

$$\begin{aligned} & \int_{\gamma_P} \psi_k(P) \int_{\Gamma_1} \frac{\partial G}{\partial\mathbf{N}}(P, Q)\mathcal{F}_1(Q) dQ dP \\ & + \int_{\gamma_P} \psi_k(P) \int_{\Gamma_2} \frac{\partial^2 G}{\partial\mathbf{N}\partial\mathbf{n}}(P, Q)\phi_2(Q) dQ dP = \int_{\gamma_P} \psi_k(P)g_2(P) dP \\ & - \int_{\gamma_P} \psi_k(P) \int_{\Gamma_1} \frac{\partial^2 G}{\partial\mathbf{N}\partial\mathbf{n}}(P, Q)g_1(Q) dQ dP \\ & - \int_{\gamma_P} \psi_k(P) \int_{\Gamma_2} \frac{\partial^2 G}{\partial\mathbf{N}}(P, Q)g_2(Q) dQ dP, \quad \gamma_P \in \Gamma_2 \end{aligned} \quad (6)$$

respectively, where  $\gamma_P$  denotes the support of the weighting function  $\psi_k(P)$ . The weighting functions are chosen to be the basis shape functions  $\psi_k$  (e.g., linear:  $\{k = 1, 2\}$ ; quadratic:  $\{k = 1, 2, 3\}$ ) employed in the approximation of  $\phi$  and  $\mathcal{F}$  on the boundary. This procedure does not by itself guarantee symmetry of the coefficient matrix, but combined with the appropriate use of the BIE and HBIE, a symmetric set of algebraic equations will be generated. This choice of equation is dictated by the symmetry properties of the kernel functions.

$$G(P, Q) = G(Q, P) \quad (7a)$$

$$\frac{\partial G}{\partial\mathbf{n}}(P, Q) = -\frac{\partial G}{\partial\mathbf{N}}(P, Q) = \frac{\partial G}{\partial\mathbf{N}}(Q, P) \quad (7b)$$

$$\frac{\partial^2 G}{\partial\mathbf{n}\partial\mathbf{N}}(P, Q) = \frac{\partial^2 G}{\partial\mathbf{n}\partial\mathbf{N}}(Q, P) \quad (7c)$$

Thus, for a Dirichlet problem, a Galerkin formulation of the BIE will produce a symmetric coefficient matrix, while the HBIE will be appropriate for a Neumann problem. The above relationships for the first derivatives of  $G$  also guarantee symmetry for a mixed boundary value problem, provided the BIE

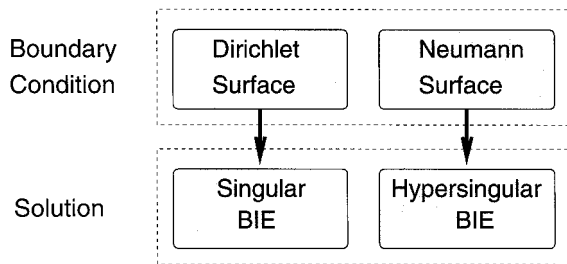


FIG. 1. Symmetric Galerkin BEM Solution Phase

is employed on  $\Gamma_1$  and the HBIE on  $\Gamma_2$ , as illustrated by Fig. 1.

After discretization, the set of (5) and (6) can be written in matrix form as

$$[A]\{w\} = \{f\} \quad (8)$$

The matrix elements are composed of double integrals, and  $P$  and  $Q$  are treated on an equal footing. Note that  $[A]$  is the symmetric system matrix obtained from the terms on the left-hand side, and  $\{f\}$  is the known right-hand side obtained from the terms on the right-hand side of both (5) and (6). Moreover, the approximate numerical solution  $\{w\}$  obtained from (8) can be decomposed as

$$w = [w_1, w_2]^T$$

where  $w_1 \equiv \mathcal{F}_1$ ,  $w_2 \equiv \phi_2$ , and  $T$  denotes the transpose of a matrix.

## GALERKIN RESIDUALS AND ERROR ESTIMATES

This work provides evidence that the ‘‘Galerkin residuals’’ reasonably estimate discretization errors in numerical solutions obtained by the SG-BEM. The key concept for obtaining the Galerkin residuals is the duality of the pair of integral integrations (i.e., standard and hypersingular BIEs), which has been described by Paulino et al. (1996). In the SG-BEM, both the standard and the hypersingular BIEs are employed, the choice being dictated by the prescribed boundary condition. The interchange in the role of the two equations is the basis for the error estimation, as illustrated by Fig. 2 (cf., Fig. 1). Thus, on the Dirichlet parts of the boundary, the error estimate  $\mathcal{E}_1(P)$  is defined as the residual that arises when the approximate solution is substituted in the HBIE.

$$\begin{aligned} \mathcal{E}_1(P) = & - \int_{\gamma_P} \psi_k(P) w_1(P) dP \\ & + \int_{\gamma_P} \psi_k(P) \int_{\Gamma_1} \frac{\partial G}{\partial \mathbf{N}}(P, Q) w_1(Q) dQ dP \\ & + \int_{\gamma_P} \psi_k(P) \int_{\Gamma_2} \frac{\partial G}{\partial \mathbf{N}}(P, Q) g_2(Q) dQ dP \\ & - \int_{\gamma_P} \psi_k(P) \int_{\Gamma_1} \frac{\partial^2 G}{\partial \mathbf{N} \partial \mathbf{n}}(P, Q) g_1(Q) dQ dP \\ & - \int_{\gamma_P} \psi_k(P) \int_{\Gamma_2} \frac{\partial^2 G}{\partial \mathbf{N} \partial \mathbf{n}}(P, Q) w_2(Q) dQ dP \end{aligned} \quad (9)$$

As the weight function is centered on the node  $P_k$  and is non-zero only on the neighborhood of this node, this is taken to be an estimate of the local error in the computed flux at this point. Similarly, on the Neumann parts of the boundary, the error estimate  $\mathcal{E}_2(P)$  is defined as the residual that arises when the approximate solution is substituted in the BIE.

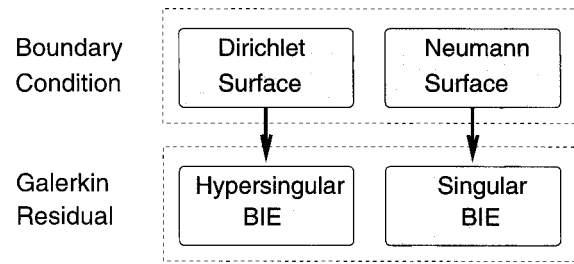


FIG. 2. Combined Singular-Hypersingular Residual Calculation Phase

$$\begin{aligned} \mathcal{E}_2(P) = & - \int_{\gamma_P} \psi_k(P) w_2(P) dP \\ & - \int_{\gamma_P} \psi_k(P) \int_{\Gamma_1} \frac{\partial G}{\partial \mathbf{n}}(P, Q) g_1(Q) dQ dP \\ & - \int_{\gamma_P} \psi_k(P) \int_{\Gamma_2} \frac{\partial G}{\partial \mathbf{n}}(P, Q) w_2(Q) dQ dP \\ & + \int_{\gamma_P} \psi_k(P) \int_{\Gamma_1} G(P, Q) w_1(Q) dQ dP \\ & + \int_{\gamma_P} \psi_k(P) \int_{\Gamma_2} G(P, Q) g_2(Q) dQ dP \end{aligned} \quad (10)$$

This is likewise interpreted as an estimate of the error in the computed value of  $\phi(P_k)$ . Moreover

$$\mathcal{E} = \mathcal{E}_1 \cup \mathcal{E}_2$$

Only the magnitude (and not the sign) of the Galerkin residuals ( $\mathcal{E}$ ) is employed in the error estimation and adaptive procedure developed below. In general, error estimates are defined in terms of appropriate norms of the residuals (e.g., Paulino et al. 1996; Szabó and Babuška 1991); in this case, only the magnitude of the residuals is needed.

## COMPUTATIONAL EFFICIENCY ISSUES

For mixed boundary value problems, the SG-BEM approximation relies on the use of both the singular and hypersingular Galerkin BIEs, i.e., (5) and (6), respectively. Issues concerning both the integration and solution phases are discussed next. As explained previously, the integrations, involving derivatives of Green’s function, are defined in the ‘‘limit to the boundary’’ sense. The integrations are performed by means of a combined analytical and numerical approach. The analytical integration allows the potentially divergent terms to be identified, and the cancellation of these terms, which must occur, is accompanied ‘‘exactly’’ rather than numerically. Much of this process can be automated using computer algebra (e.g., by taking advantage of the capabilities of a symbolic computation software such as MAPLE, developed by Waterloo Maple Software), which significantly reduces the overall effort required in the solution and implementation of boundary integral equations. This also helps with efficiency because the integrals that are computed numerically are completely nonsingular, and thus low-order Gauss quadrature can be safely invoked. Here linear elements are employed; however, integrals resulting from higher order curved interpolation can be shown to be reducible to the linear case (Gray 1993). These hybrid algorithms (i.e., analytical/numerical) are much faster than a brute-force numerical approach (Balakrishna et al. 1994).

The symmetry can be exploited in both matrix construction and solution phases to provide the efficiency needed to counterbalance the high computational cost of the extra boundary

integral equations in the Galerkin method. In general, SG is competitive with collocation and will be faster for sufficiently large problems. For example, for two-dimensional problems, the crossover point where SG becomes more efficient is known to occur around 200 to 300 elements (Balakrishna et al. 1994).

The Galerkin residuals ( $\mathcal{E}$ ) are calculated in a postprocessing stage [see (9) and (10)], i.e., after the solution of the primary boundary value problem. Thus, they lead to a posteriori error estimates. The evaluation of these residuals is also efficient because it relies on the integration procedure (hybrid analytical/numerical) discussed above.

### SELF-ADAPTIVE STRATEGY

The self-adaptive mesh refinement strategy employed in this work is the  $h$ -version, which generates a sequence of meshes of increasing refinement. The self-adaptive procedure is performed according to the flowchart of Fig. 3. The goal is to efficiently develop a well-graded final mesh, leading to a reliable numerical solution, in as simple a manner as possible. To avoid loss of numerical accuracy (Crouch and Starfield 1983; Rencis and Jong 1989; Guiggiani 1990), elements should not be graded such that large elements appear close to small elements. To solve this problem, Guiggiani (1990) has adopted an additional rule, called a compatibility condition, so that whenever the ratio between the length of two adjacent elements was out of the range 0.25 to 4.0, the longer element was bisected. Because of its arbitrariness, this type of rule has not been used in the present work. Moreover, bad mesh gradation (in the sense described above) has not occurred for the examples presented in this paper. This is a result of the quality of the error estimators using Galerkin residuals.

#### Local Error Estimation

Once the ‘‘Galerkin residuals’’ have been obtained [(9) and (10)] at each nodal point, they are normalized as

$$\bar{\mathcal{E}}_i = \left| \frac{\mathcal{E}_i}{\mathcal{E}_{\max}} \right|, \quad i = 1, \dots, n_n \quad (11)$$

where

$$\mathcal{E}_{\max} = \max(|\mathcal{E}_1|, |\mathcal{E}_2|, \dots, |\mathcal{E}_{n_n}|) \quad (12)$$

and  $n_n$  denotes the total number of nodes. In this work, linear boundary elements with shape functions

$$N_1(\xi) = 1 - \xi; \quad N_2(\xi) = \xi \quad (13a,b)$$

have been used, and  $\psi_k(\xi) = N_k(\xi)$ ,  $k = 1, 2$ . However, the error estimation method is general and is not limited to linear elements. The error indicator for the boundary element ( $i$ ) is denoted as  $\mathcal{E}^{(i)}$  and is obtained as

$$\mathcal{E}^{(i)} = L^{(i)} \int_0^1 (N_1 \bar{\mathcal{E}}_{\text{node}1}^{(i)} + N_2 \bar{\mathcal{E}}_{\text{node}2}^{(i)}) d\xi \quad (14a)$$

$$\mathcal{E}^{(i)} = L^{(i)} \frac{\bar{\mathcal{E}}_{\text{node}1}^{(i)} + \bar{\mathcal{E}}_{\text{node}2}^{(i)}}{2}, \quad i = 1, \dots, n_e \quad (14b)$$

where  $n_e$  denotes the number of elements,  $L^{(i)}$  is the element length, and  $\bar{\mathcal{E}}_{\text{node}1}^{(i)}$  and  $\bar{\mathcal{E}}_{\text{node}2}^{(i)}$  are the values of the normalized error indicators at the beginning and end nodes of the boundary element ( $i$ ).

#### Element Refinement Criterion

A simple criterion for mesh refinement consists of bisecting the element for which its error indicator is larger than a reference value. Here, this reference quantity is taken as the average error indicator given by

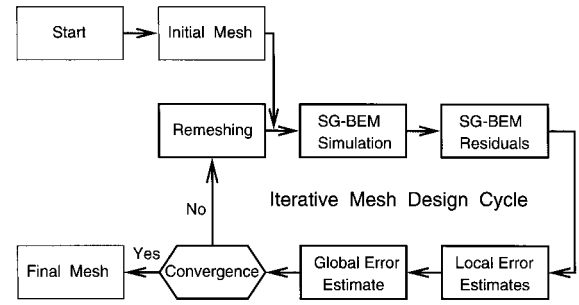


FIG. 3. Self-Adaptive Analysis Algorithm ( $h$ -Version)

$$\mathcal{E}_{\text{ref}} = \frac{1}{n_e} \sum_{i=1}^{n_e} \mathcal{E}^{(i)} \quad (15)$$

If the inequality

$$\mathcal{E}^{(i)} > \gamma \mathcal{E}_{\text{ref}}, \quad i = 1, \dots, n_e \quad (16)$$

is satisfied, then the element is divided into two elements (bisection). The parameter  $\gamma$  in (16) is a weighting coefficient that allows one to control the ‘‘refining velocity.’’ The standard procedure consists of using  $\gamma = 1$ . Cases where  $\gamma \neq 1$  are discussed next.

If  $\gamma > 1$ , then the number of elements to be refined is less than with  $\gamma = 1$ . By selecting  $\gamma > 1$ , one can control the total number of elements at each step and avoid too many refinements. The numerical solution from the next step (Fig. 3) is expected to be more accurate than that of the current step; however, the increase on the total number of elements is comparatively smaller. This approach is useful when the total number of elements is expected to be less than a certain number. The disadvantage is that the convergence rate is slower than that with  $\gamma = 1$ .

If  $\gamma < 1$ , the number of elements to be refined is larger than with  $\gamma = 1$ . The advantage is that the refinement rate should increase. However, the computational efficiency would decrease owing to the likely generation of an excessive number of elements.

#### Global Error Estimation

The adaptive mesh refinement process is carried out iteratively (Fig. 3). Although the refinement may be terminated by restrictions on storage and computing time, the stopping criterion is generally a specified level of accuracy. In this case, one may be interested either in the global error of the approximation or in a pointwise error bound.

An indication of the overall convergence may be obtained by

$$\mathcal{E}_{\text{global}} = \sum_{i=1}^{n_e} \mathcal{E}^{(i)} \quad (17)$$

or

$$\mathcal{E}_{\text{global}} = \mathcal{E}_{\text{ref}} \quad (18)$$

Both (17) and (18) can be very easily obtained. The goal of the adaptive procedure is to obtain well-distributed meshes (i.e., near optimal). Ideally, as the iterative meshing progresses, the error estimates should decrease both locally and globally.

#### CORNERS

With Galerkin, the flexibility provided by the choice of weight function allows a simple and elegant corner treatment (de Paula and Telles 1989). Corners are represented by ‘‘double nodes,’’ where two distinct weight functions are used. Each weight function is ‘‘half of’’ the usual weight—it is

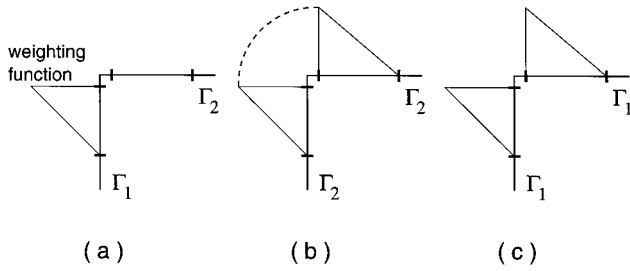


**FIG. 4. Weighting Functions ( $\psi_k$ ) for Symmetric Galerkin Method at Corners: (a) Mixed Corner (Unknown Is  $\mathcal{F}$  at  $\Gamma_1$ ); (b) Neumann Corner (Unknown Is  $\phi$  at Corner); (c) Dirichlet Corner (Unknowns Are  $\mathcal{F}$ s on Each Side of Corner)**

nonzero only on one side of the corner. If flux is specified on both sides of the corner, so that the only unknown is potential, the weight functions will be combined back into one. Otherwise, they remain separate.

The corner treatment for the error estimation is handled similarly and is illustrated in Fig. 4. For a mixed corner (i.e., corner with a Dirichlet condition on one side and a Neumann condition on the other side), only one error value is assigned at the corner. This value is associated with the error in the computed flux at the Dirichlet node. For a Neumann corner, the estimator computes a single value, again rejoining the shape functions around the corner, associated with the error in the computed potential. For a Dirichlet corner, the Galerkin code computes two flux values and two corresponding error estimates. Dirichlet corners are not common, but they do occur in applications.

## NUMERICAL EXAMPLES

As noted above, for testing purposes, we have employed a standard isoparametric linear element symmetric-Galerkin algorithm. Thus, linear shape functions are used for interpolating potential and flux, and for the weighting functions in the SG-BIEs (5) and (6).

The solution algorithm for adaptive meshing is summarized below.

1. Solve (5) and (6) simultaneously (in discretized form) to obtain the unknown values of potential and flux on the boundary.
2. In a postprocessing stage, calculate the ‘‘Galerkin residuals’’ at the nodal points by means of (9) and (10).
3. Compute element nodal errors using (14).
4. Compute average error indicator using (15).
5. Perform element refinement according to the criterion of (16).
6. Check global stopping criterion with reference to  $\mathcal{E}_{\text{global}}$  given by, for example, 18. If the global stopping criterion is satisfied, then stop. Otherwise, repeat steps 1 to 5.

Three examples are considered here:

- Rectangular region with discontinuous boundary conditions
- Transformer coil
- Eccentric annulus

These examples include mixed boundary conditions, corners, and nonconvex domains. These features are important for testing and validating the adaptive algorithm.

### Rectangular Region with Discontinuous Boundary Conditions

Figs. 5(a and b) show the rectangular geometry and the applied boundary conditions, respectively, for the first test

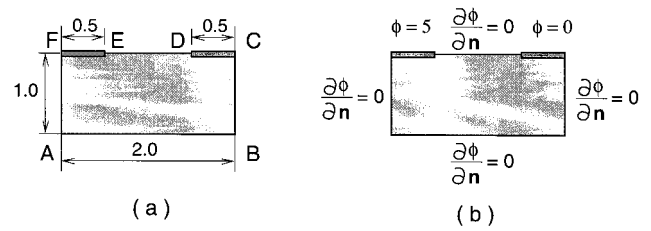


**FIG. 5. Rectangular Region: (a) Geometry; (b) Boundary Conditions**

**TABLE 1. Element Error Indicators for the Rectangular Region Problem**

Section	Mesh 1	Mesh 2	Mesh 3	Mesh 4	Mesh 5
AB	0.00235	0.00363	0.00495	0.00665	0.00960
	0.00124	0.00192	0.00300	0.00519	0.00824
	0.00122	0.00189	0.00295	0.00516	0.00810
	0.00233	0.00360	0.00490	0.00662	0.00956
BC	0.00524	0.00843	0.01089	0.00847	0.00995
	0.01847	0.01619	0.02080	0.00393 0.00241	0.00129 0.00230
CD	0.02704	0.01351	0.01229	0.00202	0.00166
	0.07020	0.01634	0.00756	0.00440	0.00294
		0.04011	0.00870	0.00368	0.00254
			0.02149	0.00453	0.00197
DE	0.10069	0.06059	0.03139	0.01585	0.00796
			0.00212	0.00066	0.00018
		0.00429	0.00138	0.00116	0.00037
	0.10072	0.00429	0.00137	0.00125	0.00095
EF		0.06060	0.00211	0.00115	0.00102
			0.03139	0.00066	0.00037
				0.01586	0.00018
					0.00796
FA	0.07031	0.04009	0.02146	0.01111	0.00566
			0.00866	0.00450	0.00230
		0.01640	0.00767	0.00365	0.00194
	0.02703	0.01355	0.01237	0.00442	0.00252
SUM	0.01833	0.01599	0.02051	0.00213	0.00195
	0.00529	0.00849	0.01099	0.00397	0.00139
SUM / n <sub>e</sub>	0.03218	0.01742	0.01132	0.00850	0.00144
					0.00095

case. This problem has been studied by Shi et al. (1995) in an  $h$ -adaptive BEM procedure (collocation based) for potential problems using linear elements and mesh sensitivities as error indicators. In their adaptive procedure, they must ‘‘maintain an even number of elements on each smooth section of the boundary’’ (Shi et al. 1995, p. 386). This restriction is not present in this work.

The initial mesh discretization, consisting of 14 elements, is the same as the one adopted by Shi et al. (1995). Table 1 shows the element error indicator, (14), map during the first four refinement steps of the adaptive procedure. The last two lines of this table provide the global errors, as given by (17) and (18), respectively. Both global error measures are monotonically decreasing with mesh refinement. The corresponding meshes, shown in Fig. 6, display a smooth mesh gradation at each iteration. The difficult areas for the calculation are the geometrical corners and the neighborhood of points D and E, where there is a discontinuity in the flux. Note that the meshes in these regions are progressively refined. The number of elements at the first four refinement steps are 14, 18, 22, 30, and 40. Shi et al. (1995) attempted two solutions for this problem with three refinement steps in each solution. For the first solution, the number of elements at each step was 14, 26, 42,

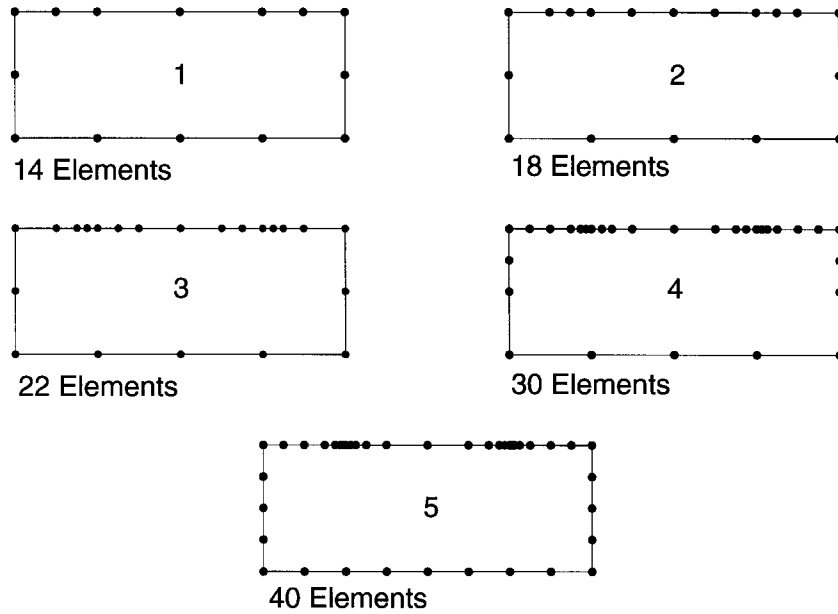


FIG. 6. Adapted Meshes for Rectangular Region Problem (First Four Refinement Steps)

and 56; and for the second solution, the number of elements at each step was 14, 24, 32, and 40. They have pointed out that the second solution leads to an improved convergence rate. The final mesh (i.e., mesh 5), shown in Fig. 6, has the same number of elements (i.e., 40) and a similar element distribution to the final mesh obtained by Shi et al. (1995) in their second solution for this problem.

As there is no analytical solution available for this problem (Fig. 5), the reference mesh, shown in Fig. 7, is used to assess the quality of the numerical solution obtained with the adaptive SG-BEM. The comparison of the solution obtained at each step (Fig. 6) with an approximate reference solution (Fig. 7) is given in Figs. 8–13. These graphs show that the numerical solution improves consistently as the mesh is refined; i.e., the solution for mesh  $i$  is better than the solution for mesh  $i - 1$

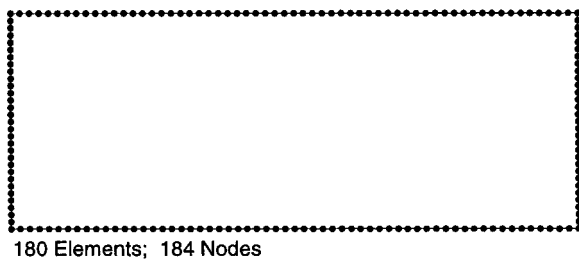


FIG. 7. Reference Mesh for Rectangular Geometry with Discontinuous Boundary Conditions

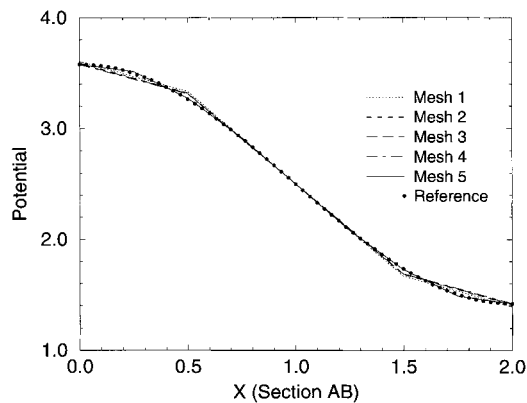


FIG. 8. Potential on Section AB

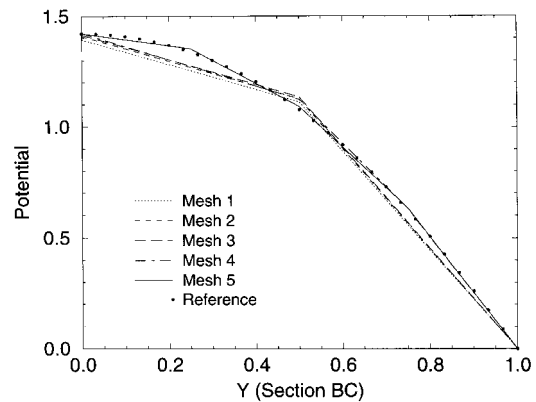


FIG. 9. Potential on Section BC

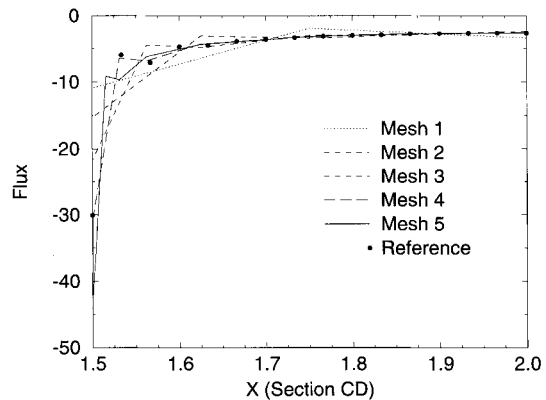


FIG. 10. Flux on Section CD [No Special Treatment of Discontinuity Condition at Point D ( $X = 1.5$ ) for Either the "Reference" Mesh or Meshes 1 to 5]

( $i = 2, \dots, 5$ ). In the present problem, points D and E (Fig. 5) are of special interest because there is a discontinuity in the value of the flux from a nonzero value on the Dirichlet sides (CD and EF) to a zero value on the Neumann side (DE). The oscillations in the flux distribution on CD (near point D) and on EF (near point E) are expected because there is no special treatment of the discontinuity condition at points D and E. Thus, the reference mesh data in Figs. 10 and 12 should be considered with caution because the discontinuity condition

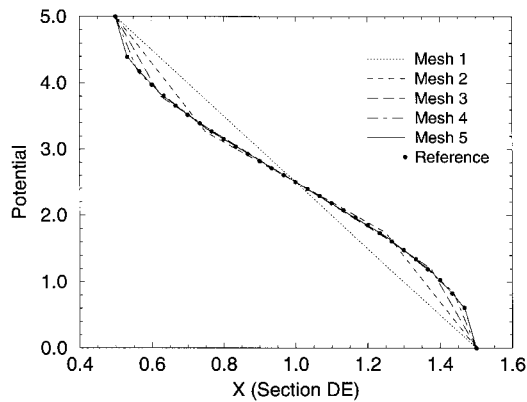


FIG. 11. Potential on Section DE

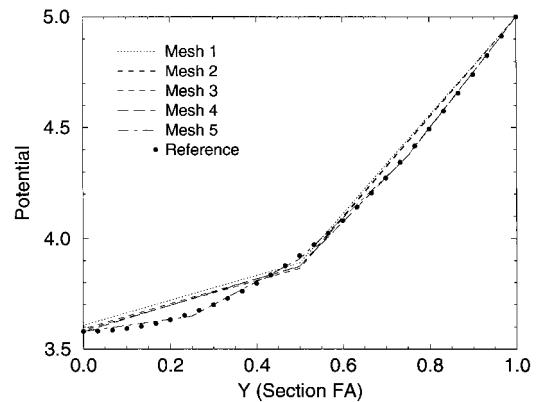


FIG. 13. Potential on Section FA

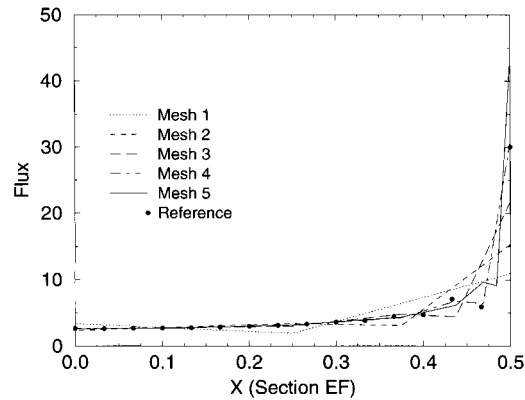


FIG. 12. Flux on Section EF [No Special Treatment of Discontinuity Condition at Point E ( $X = 0.5$ ) for Either the “Reference” Mesh or Meshes 1 to 5]

has not been treated in the numerical scheme. Nevertheless, from the graphs of Figs. 10 and 12, note that the oscillations are localized and the flux decreases rapidly away from points D (toward C) and E (toward F).

### Eccentric Annulus

The second example models heat conduction in an eccentric annulus geometry. This problem has characteristics that make it very suitable for testing purposes, e.g., curved boundaries, nonconvex region, and corners. Fig. 14 shows the geometry and boundary conditions. There is a closed-form solution for this problem, obtained by means of conformal mapping and complex variable techniques, given by [see, for example, the book by Greenberg (1978)]

$$\phi = 100 \left[ 1 - \frac{\ln(u^2 + v^2)}{2 \ln a} \right], \quad a = 2 + \sqrt{3} \quad (19)$$

where

$$u(x, y) = \frac{(ax - 1)(x - a) + ay^2}{(ax - 1)^2 + a^2y^2} \quad (20a)$$

$$v(x, y) = \frac{(a^2 - 1)y}{(ax - 1)^2 + a^2y^2} \quad (20b)$$

For this problem, one can take advantage of symmetry and model only the top (or bottom) part of the problem. This approach is followed here, and only the top part of the annulus [Fig. 14(b)] is considered in the adaptive analysis. Note that, when symmetry is used, the discretization error is greater than when symmetry is not employed since elements are placed on the symmetry axis. Also, by using the symmetry, the problem becomes a mixed boundary value problem.

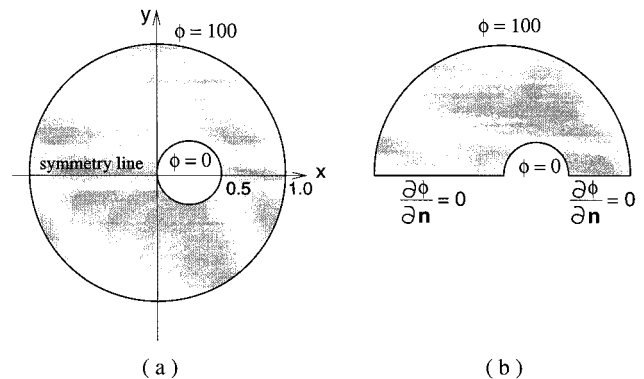


FIG. 14. Eccentric Annulus: (a) Geometry; (b) Boundary Conditions

The sequence of meshes obtained during the self-adaptive mesh refinement procedure is given in Fig. 15. A well-graded mesh (i.e., mesh 5) is generated in four iterative steps. Note that this mesh possesses well-distributed elements with a strong gradation at the corners. Comparison of the theoretical solution provided by (19) and (20) with the SG-BEM solution reveals that the maximum relative error is 3.62% (for the node at  $146.25^\circ$ , counterclockwise, on the top semicircle with radius 0.25); however, for most nodal points the error is much less than 1%. Moreover, the numerical results obtained with this mesh are practically the same as those reported by Gray and Paulino (1997, tables 2–5). However, in that reference, the problem is modeled using a double region in order to validate a symmetric Galerkin multizone formulation, and here it is modeled using a single region [Fig. 14(b)].

Table 2 shows the values of the two global error estimators given by (17) and (18) for each of the meshes in Fig. 15. Again, both estimates monotonically decrease with the number of elements.

### Transformer Coil

This last example considers heat conduction in a transformer coil. Fig. 16 shows the geometry and boundary conditions. This problem has been studied by Rencis and Jong (1989a,b) in an early BEM adaptive procedure ( $h$ -version) for potential problems. Their analysis employed constant elements and a projection process of adjacent boundary element solutions as an error estimate. The modeling of this problem with linear elements involves 12 corners, of which 2 are of the Dirichlet type, 8 are of the Neumann type, and 2 are mixed.

The initial mesh, with 20 linear elements, is similar to the one adopted by Rencis and Jong (1989a, figure 11, p. 311). They started (see the “mesh points”) with an initial mesh containing 18 elements and reached an adapted mesh with 68

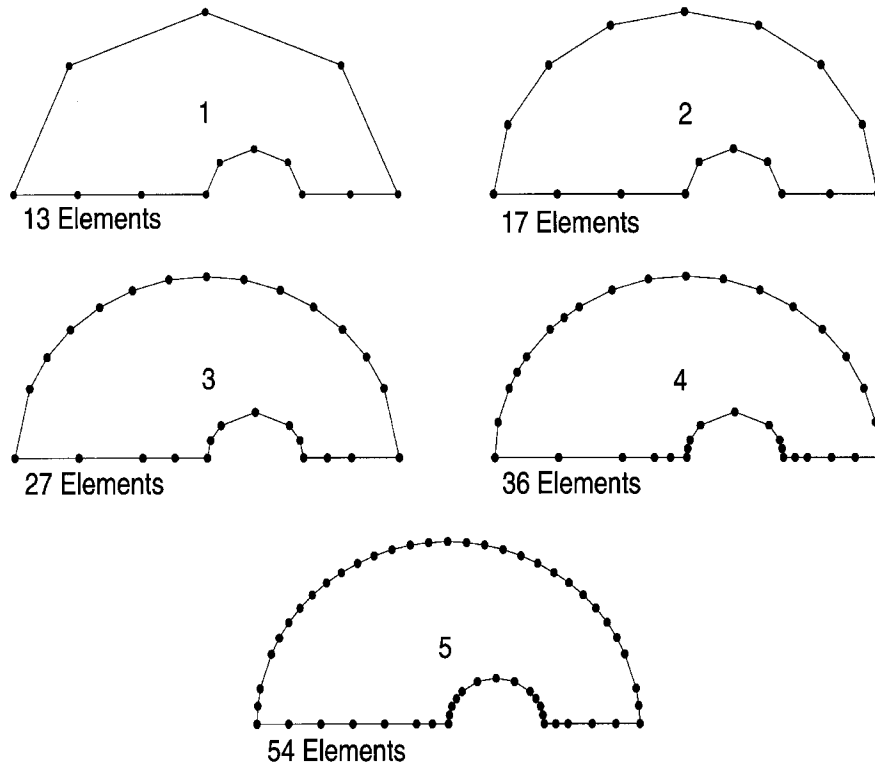


FIG. 15. Adapted Meshes for Eccentric Annulus Problem (First Four Refinement Steps)

TABLE 2. Global Error Estimates for Eccentric Annulus Problem

Mesh (1)	$n_e$ (2)	Global Estimates	
		Eq. (17) (3)	Eq. (18) (4)
1	13	3.19378	0.24568
2	17	1.81541	0.10679
3	27	1.59126	0.05894
4	36	1.18794	0.03300
5	54	0.75659	0.01401

elements. The meshes obtained in the present adaptive refinement are given in Fig. 17. This procedure yields a well-graded mesh (i.e., mesh 5) in four iterative steps.

The corresponding system matrix  $[A]$  [see (8)] to each of the five meshes in Fig. 17 is given in Figs. 18–22. Note that the overall matrix pattern converges to the pattern of the last iteration (Fig. 22). From a qualitative point of view, the matrix in Fig. 22 displays the strongest diagonal dominance when compared to the previous matrix patterns (i.e.,  $[A]_{\text{Mesh } 1}$  to  $[A]_{\text{Mesh } 4}$  in Figs. 18–21, respectively). [The reader is referred to the book by Stoer and Bulirsch (1993) for the mathematical definition of “diagonal dominance” of a matrix.] Moreover, the range of values of the entries in the system matrices change slowly from the first matrix (Fig. 18) to the fourth one (Fig. 21), and it stabilizes afterwards, as can be verified in Fig. 22.

There is once again no analytical solution available for this problem, and thus a reference mesh with 240 elements, shown in Fig. 23, has been used to evaluate the accuracy of the solutions. The temperature distribution on the Neumann part of the boundary, i.e., along sides  $B \cdots K$  in Fig. 16(a) is of special interest because of high temperature gradients, especially along the edges EF and GH. Fig. 24 shows the temperature distribution along the arc length  $B \cdots K$ , which indicates that the solutions obtained with the fourth and fifth meshes are quite close to the reference solution. Fig. 25 presents the nodal residual distribution along the arc length  $B \cdots K$ . As

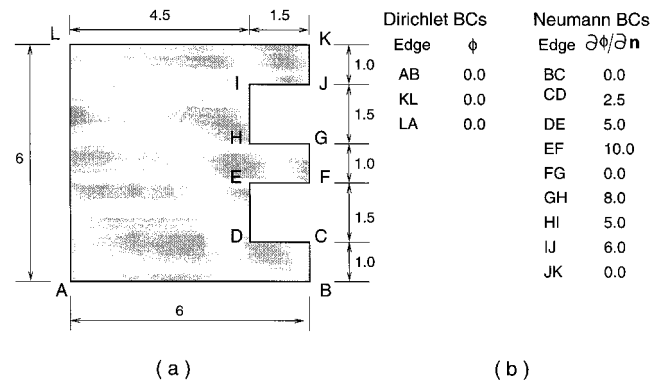


FIG. 16. Transformer Coil: (a) Geometry; (b) Boundary Conditions

expected, the magnitudes of the residuals decrease as the mesh is refined. Moreover, this plot also shows a good convergence rate of the residual, in the sequence of adapted meshes, toward the residual of the reference mesh.

## CONCLUSIONS AND EXTENSIONS

A simple and effective “a posteriori” error estimation method for the symmetric Galerkin boundary element method has been developed and coupled with an  $h$ -adaptive strategy. The error estimation method employs “Galerkin residuals” and is based upon the use of both the standard BIE and the hypersingular BIE. This is a natural idea for the symmetric Galerkin methodology, as this method already utilizes both equations to solve the boundary value problem. Thus, the computational implementation into an existing SG-BEM code structure is straightforward as both equations (i.e., BIE and HBIE) are already available as part of the primary computer code. Moreover, with Galerkin the hypersingular equation can be correctly approximated with standard continuous elements.

Three numerical examples, with various features (e.g., mixed boundary conditions, nonconvex domains, and corners)

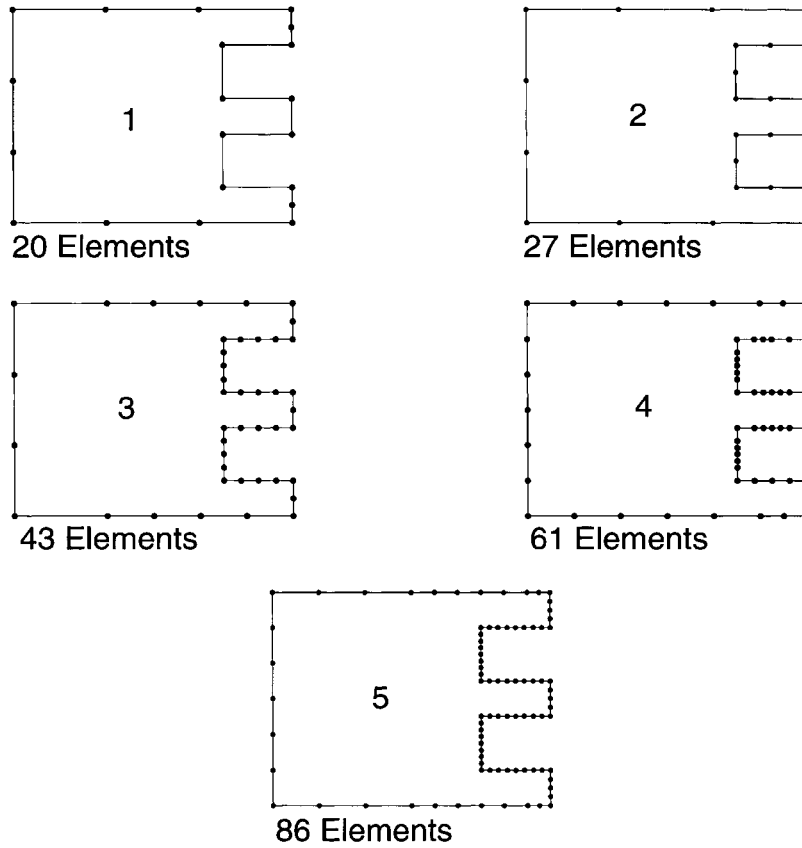


FIG. 17. Adapted Meshes for Transformer Coil Problem (First Four Refinement Steps)

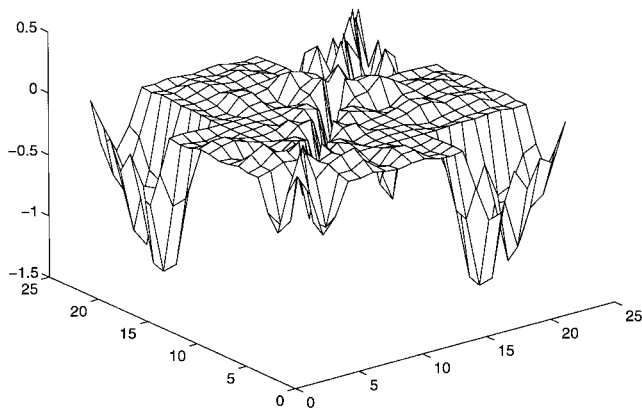


FIG. 18. System Matrix  $[A]_{\text{Mesh1}}$ : Axes are  $n_e \times n_e \times$  (Entry - Value)

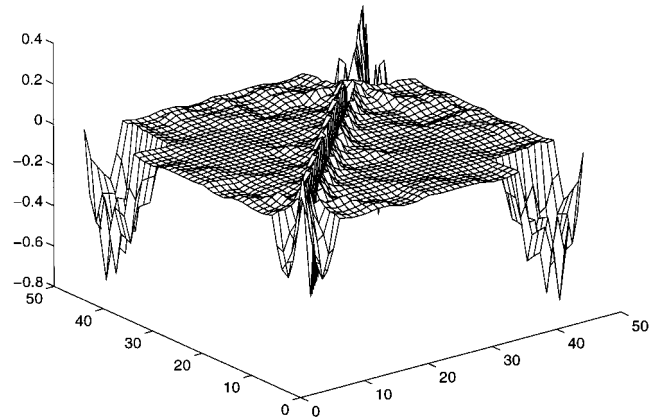


FIG. 20. System Matrix  $[A]_{\text{Mesh3}}$ : Axes are  $n_e \times n_e \times$  (Entry - Value)

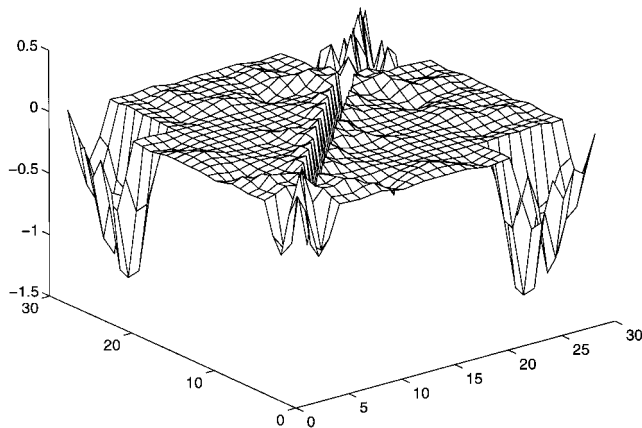


FIG. 19. System Matrix  $[A]_{\text{Mesh2}}$ : Axes are  $n_e \times n_e \times$  (Entry - Value)

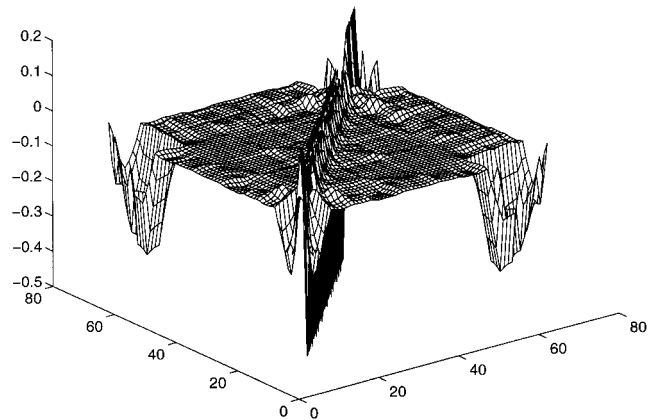


FIG. 21. System Matrix  $[A]_{\text{Mesh4}}$ : Axes are  $n_e \times n_e \times$  (Entry - Value)

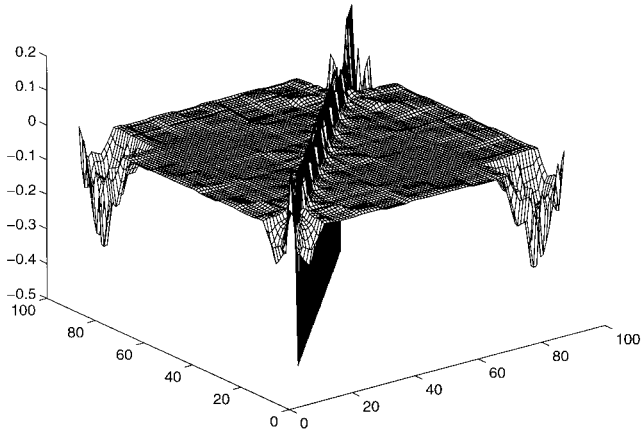


FIG. 22. System Matrix  $[A]_{\text{Mesh 5}}$ : Axes are  $n_e \times n_e \times (\text{Entry} - \text{Value})$

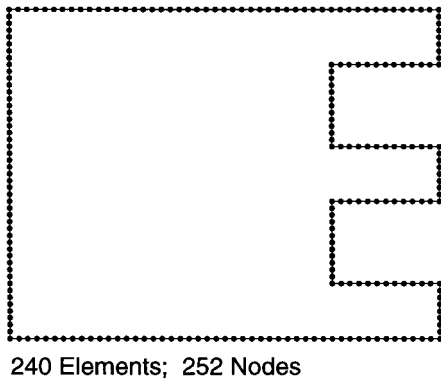


FIG. 23. Reference Mesh for Transformer Coil

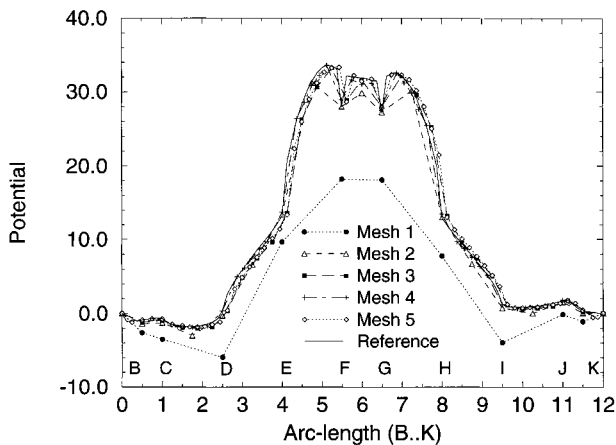


FIG. 24. Potential along Arc Length  $B \cdots K$

for testing and validating the SG-BEM adaptive procedure have been presented. For these examples, it is fair to say that the final meshes obtained (Figs. 6, 15, and 17) are close to the ones that an experienced engineer would use. However, since the proposed procedure is automated, it does not require the engineer to carry out the usual manual remeshing process. The user is required only to define an initial mesh and a certain accuracy tolerance.

For all the examples in this paper, a converged solution (according to the adopted self-adaptive method) has been obtained in a few steps, for instance, fewer than five iterations. To improve computational efficiency and to reduce the number of trial solutions, two approaches are being investigated. First, the element refinement criterion used here is based on bisection of elements, and thus for initial elements with high error, multiple iterations are required to subdivide this element ap-

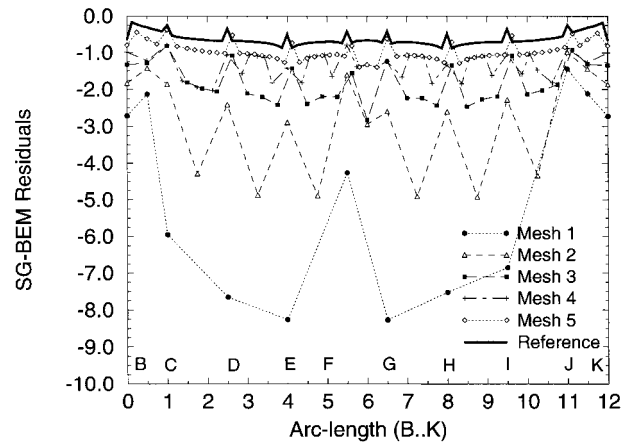


FIG. 25. SG-BEM Residuals at Nodes along Arc Length  $B \cdots K$

propriately. It would therefore be desirable to define a refinement criterion that specifies whether an element should be partitioned into two or more parts. [See, for example, the book by Zienkiewicz and Taylor (1989, chapter 14) and the article by Krishnamoorthy and Umesh (1993) for use of this concept in an FEM context.] This idea should be considered together with requirements to guarantee a well-graded boundary element mesh. Ideally, a final mesh should be obtained in just one (preferably) or two iterations.

Second, evaluating the residual at the point  $P_0$  by means of either (9) or (10) involves a costly integration over the entire boundary. As  $\mathcal{E}(P_0)$  is by nature only an estimate, it should suffice to do the calculation approximately, and one possibility is to neglect “far-field” integrals by truncating the calculation at some specified distance from point  $P_0$ . This would significantly reduce the computational cost of obtaining the error estimates. Other techniques to be considered for improved computational efficiency include the use of iterative solvers and multigrid solutions.

This work has been in the context of the two-dimensional Laplace equation using linear Galerkin boundary elements. However, the idea presented here extends naturally to higher order elements (e.g., quadratic), vector-field (e.g., elasticity), and three-dimensional problems. Interesting areas of investigation consist of extending the present method to other linear-type problems such as multizone and fracture mechanics, and to nonlinear material behavior such as plasticity problems. These are topics for future research.

## ACKNOWLEDGMENTS

The first writer acknowledges support from the National Science Foundation under Grant CMS-9713008. The second writer was supported by the Applied Mathematical Sciences Research Program of the Office of Mathematical, Information, and Computational Sciences, U.S. Department of Energy, under contract DE-AC05-96OR22464 with Lockheed Martin Energy Research Corp. Additional support from the National Science Foundation under Grant PHY94-07194 with the Institute for Theoretical Physics, University of California, Santa Barbara, is also gratefully acknowledged. The writers thank Jason L. Kintzel for helping with the numerical examples in this work.

## APPENDIX. REFERENCES

- Abe, K. (1992). “A new residue and nodal error evaluation in  $h$ -adaptive boundary element method.” *Adv. Engrg. Software*, 15(3/4), 231–239.
- Balakrishna, C., Gray, L. J., and Kane, J. H. (1994). “Efficient analytical integration of symmetric Galerkin boundary integrals over curved elements: Thermal conduction formulation.” *Comput. Methods Appl. Mech. Engrg.*, 111(3–4), 335–355.
- Banerjee, P. K. (1994). *The boundary element methods in engineering*, 2nd Ed., McGraw-Hill, London.
- Becker, A. A. (1992). *The boundary element method in engineering*, McGraw-Hill, London.

- Brebbia, C. A., Telles, J. C. F., and Wrobel, L. C. (1984). *Boundary element techniques*. Springer-Verlag, Berlin and New York, 1984.
- Carstensen, C. (1995). "Adaptive boundary element methods and adaptive finite element methods and boundary element coupling." *Boundary value problems and integral equations in nonsmooth domains*, M. Costabel, M. Dauge, and S. Nicaise, eds., Marcel Dekker, Inc., New York, 47–58.
- Carstensen, C. (1996). "Efficiency of a posteriori BEM error estimates for first kind integral equations on quasi-uniform meshes." *Math. Comput.*, 65(213), 69–84.
- Carstensen, C., Estep, D., and Stephan, P. (1995). "*h*-adaptive boundary element schemes." *Computational Mech.*, 15(4), 372–383.
- Carstensen, C., and Stephan, E. P. (1995). "A posteriori error estimates for boundary element methods." *Math. Comput.*, 64(210), 483–500.
- Crouch, S. L., and Starfield, A. M. (1983). *Boundary element methods in solid mechanics*. George Allen & Unwin, London.
- Cruse, T. A., and Richardson, J. D. (1997). "Non-singular Somigliana stress identities in elasticity." *Int. J. Numer. Methods in Engrg.*, 39(19), 3273–3304.
- de Paula, F. A., and Telles, J. C. F. (1989). "A comparison between point collocation and Galerkin for stiffness matrices obtained by boundary elements." *Engrg. Anal. Boundary Elem.*, 6(3), 123–128.
- Eriksson, K., Estep, D., Hansbo, P., and Johnson, C. (1995). "Introduction to adaptive methods for differential equations." *Acta Numerica 1995*, A. Iserles, ed., Cambridge University Press, London and New York, chapter 3, 105–158.
- Ghosh, N., Rajiyah, H., Ghosh, S., and Mukherjee, S. (1986). "A new boundary element method formulation for linear elasticity." *J. Appl. Mech. Trans. ASME*, 53(1), 69–76.
- Gray, L. J. (1989). "Boundary element method for regions with thin internal cavities." *Engrg. Anal. Boundary Elem.*, 6(4), 180–184.
- Gray, L. J. (1993). "Symbolic computation of hypersingular boundary integrals." *Advances in boundary element techniques*, J. H. Kane, G. Maier, N. Tosaka, and S. N. Atluri, eds., Springer-Verlag, Berlin and Heidelberg, chapter 8, 157–172.
- Gray, L. J., Martha, L. F., and Inghraffa, A. R. (1990). "Hypersingular integrals in boundary element fracture analysis." *Int. J. Numer. Methods in Engrg.*, 29(6), 1135–1158.
- Gray, L. J., and Paulino, G. H. (1997). "Symmetric Galerkin boundary integral formulation for interface and multi-zone problems." *Int. J. Numer. Methods in Engrg.*, 40(16), 3085–3101.
- Greenberg, M. D. (1978). *Foundations of applied mathematics*. Prentice-Hall, Englewood Cliffs, N.J.
- Guiggiani, M. (1990). "Error indicators for adaptive mesh refinement in the boundary element method—A new approach." *Int. J. Numer. Methods in Engrg.*, 29(6), 1247–1269.
- Hall, W. S., and Hibbs, T. T. (1988). "The treatment of singularities and the application of the Overhauser  $C^{(1)}$  continuous quadrilateral boundary elements to three dimensional elastostatics." *Advanced boundary element methods*, T. A. Cruse, ed., Vol. 16, Springer-Verlag, Berlin and Heidelberg, 135–144.
- Hartmann, F., Katz, C., and Protosaltis, B. (1985). "Boundary elements and symmetry." *Ing.-Arch.*, 55(6), 440–449.
- Holzer, S. M. (1994). "A *p*-extension of the symmetric boundary element method." *Comput. Methods Appl. Mech. Engrg.*, 115(3–4), 339–357.
- Holzer, S. M. (1995). "The *h*-, *p*- and *hp*-versions of the BEM in elasticity: Numerical results." *Commun. Numer. Methods Engrg.*, 11(3), 255–265.
- Kita, E., and Kamiya, N. (1994). "Recent studies on adaptive boundary element methods." *Adv. Engrg. Software*, 19(1), 21–32.
- Krishnamoorthy, C. S., and Umesh, K. R. (1993). "Adaptive mesh refinement for two-dimensional finite element stress analysis." *Comput. Struct.*, 48(1), 121–133.
- Liapis, S. (1995). "A review of error estimation and adaptivity in the boundary element method." *Engrg. Anal. Boundary Elem.*, 14(4), 315–323.
- Mackerle, J. (1993). "Mesh generation and refinement for FEM and BEM—A bibliography (1990–1993)." *Finite Elem. Anal. Design*, 15(2), 177–188.
- Mackerle, J. (1994). "Error analysis, adaptive techniques and finite and boundary elements—A bibliography (1992–1993)." *Finite Elem. Anal. Design*, 17(3), 231–246.
- Martin, P. A., and Rizzo, F. J. (1996). "Hypersingular integrals: How smooth must the density be?" *Int. J. Numer. Methods in Engrg.*, 39(4), 687–704.
- Menon, G. (1996). "Hypersingular error estimates in boundary element methods." MS thesis, Cornell University, Ithaca, N.Y.
- Nagarajan, A., Mukherjee, S., and Lutz, E. (1996). "The boundary contour method for three-dimensional linear elasticity." *J. App. Mech. Trans. ASME*, 63, 278–286.
- Parreira, P., and Dong, Y. F. (1992). "Adaptive hierarchical boundary elements." *Adv. Engrg. Software*, 15(3/4), 249–259.
- Paulino, G. H. (1995). "Novel formulations of the boundary element method for fracture mechanics and error estimation." PhD thesis, Cornell University, Ithaca, N.Y.
- Paulino, G. H., Gray, L. J., and Zarijian, V. (1996). "Hypersingular residuals—A new approach for error estimation in the boundary element method." *Int. J. Numer. Methods in Engrg.*, 36(12), 2005–2029.
- Paulino, G. H., Shi, F., Mukherjee, S., and Ramesh, P. (1997). "Nodal sensitivities as error estimates in computational mechanics." *Acta Mechanica*, 121(1–4), 191–213.
- Postell, F. V., and Stephan, E. P. (1990). "On the *h*-, *p*- and *h-p* versions of the boundary element method—numerical results." *Comput. Methods Appl. Mech. Engrg.*, 83(1), 69–89.
- Rank, E. (1989). "Adaptive *h*-, *p*- and *hp*-versions for boundary integral element methods." *Int. J. Numer. Methods in Engrg.*, 28(6), 1335–1349.
- Rencis, J. J., and Jong, K.-Y. (1989a). "Error estimation for boundary element analysis." *J. Engrg. Mech.*, ASCE, 115(9), 1993–2010.
- Rencis, J. J., and Jong, K.-Y. (1989b). "A self-adaptive *h*-refinement technique for the boundary element method." *Comput. Methods Appl. Mech. Engrg.*, 73, 295–316.
- Rudolph, T. J., and Muci-Küchler, K. H. (1991). "Consistent regularization of both kernels in hypersingular integral equations." *Boundary Elements XIII*, C. A. Brebbia and G. S. Gipson, eds., Southampton and Boston, Computational Mechanics Publications and Elsevier, 875–887.
- Selcuk, S., Hurd, D. S., Crouch, S. L., and Gerberich, W. W. (1994). "Prediction of interfacial crack path: A direct boundary integral approach and experimental study." *Int. J. Fract.*, 67(1), 1–20.
- Shi, F., Ramesh, P., and Mukherjee, S. (1995). "Adaptive mesh refinement of the boundary element method for potential problems by using mesh sensitivities as error indicators." *Computational Mech.*, 16(6), 379–395.
- Sirtori, S., Maier, G., Novati, G., and Miccoli, S. (1992). "A Galerkin symmetric boundary-element method in elasticity: Formulation and implementation." *Int. J. Numer. Methods in Engrg.*, 35(2), 255–282.
- Sloan, I. H. (1990). "Superconvergence." *Numerical solution in integral equations*, M. A. Golberg, ed., Plenum Press, New York, chapter 2, 35–70.
- Sloan, I. H. (1992). "Error analysis of boundary integral methods." *Acta Numerica*, A. Iserles, ed., Cambridge University Press, London and New York, chapter 7, 287–339.
- Stoer, J., and Bulirsch, R. (1993). *Introduction to numerical analysis*, 2nd Ed., Springer-Verlag, New York.
- Sun, W., and Zamani, N. G. (1992). "An adaptive *h-r* boundary element algorithm for the Laplace equation." *Int. J. Numer. Methods in Engrg.*, 33(3), 537–552.
- Szabó, B., and Babuška, I. (1991). *Finite element analysis*. Wiley, New York.
- Tomlinson, K., Bradley, C., and Pullan, A. (1996). "On the choice of a derivative boundary element formulation using Hermite interpolation." *Int. J. Numer. Methods in Engrg.*, 39(3), 451–468.
- Watson, J. O. (1936). "Hermitian cubic and singular elements for plane strain." *Developments in boundary element methods*, P. K. Banerjee and J. O. Watson, eds., Vol. 4, Elsevier Applied Science, London and New York, chapter 1, 1–28.
- Wendland, W. L., and Yu, D.-H. (1988). "Adaptive boundary element methods for strongly elliptic integral equations." *Numer. Math.*, 53, 539–558.
- Wendland, W. L., and Yu, D.-H. (1992). "A-posteriori local error estimates of boundary element methods with some pseudo-differential equations on closed curves." *J. Comput. Math.*, 10(3), 273–289.
- Yu, D.-H. (1987). "A posteriori error estimates and adaptive approaches for some boundary element methods." *Mathematical and computational aspects*, C. Brebbia, W. L. Wendland, and G. Kuhn, eds., Vol. 1 of *Boundary elements IX*, Computational Mechanics Publications, Springer-Verlag, New York, 241–256.
- Yu, D.-H. (1988). "Self-adaptive boundary element methods." *Z. Angew. Math. Mech.*, 68(5), T435–T437.
- Yu, D.-H. (1991). "Mathematical foundation of adaptive boundary element methods." *Comput. Methods Appl. Mech. Engrg.*, 91(1–3), 1237–1243.
- Zienkiewicz, O. C., and Taylor, R. L. (1989). *The finite element method—Basic formulation and linear problems*, Vol. 1, McGraw-Hill, London.